Deficiency in *AK9* causes asthenozoospermia and male infertility by destabilising sperm nucleotide homeostasis

Yanwei Sha,[a,b,c,h] Wensheng Liu,[d,h] Shu Li,[b,h] Ludmila V. Osadchuk,[e] Yongjie Chen,[f] Hua Nie,[d] Shuai Gao,[b] Linna Xie,[c] Weibing Qin,[d,***] Huiliang Zhou,[g,**] and Lin Li[f,*]

[a]Department of Andrology, Women and Children's Hospital, School of Medicine, Xiamen University, Xiamen, Fujian, China
[b]Fujian Provincial Key Laboratory of Reproductive Health Research, School of Medicine, Xiamen University, Xiamen, Fujian, China
[c]State Key Laboratory of Molecular Vaccinology and Molecular Diagnostics, School of Public Health, Xiamen University, Xiamen, Fujian, China
[d]NHC Key Laboratory of Male Reproduction and Genetics, Guangdong Provincial Reproductive Science Institute (Guangdong Provincial Fertility Hospital), Guangzhou, Guangdong, China
[e]The Federal Research Center Institute of Cytology and Genetics, Siberian Branch of the Russian Academy of Sciences, Novosibirsk, Russia
[f]Central Laboratory, Beijing Obstetrics and Gynecology Hospital, Capital Medical University, Beijing Maternal and Child Health Care Hospital, Dongcheng, Beijing, China
[g]Department of Andrology, First Affiliated Hospital of Fujian Medical University, No.20, Chazhong Road, Fuzhou, Fujian, China

eBioMedicine
2023;96: 104798
Published Online xxx
https://doi.org/10.1016/j.ebiom.2023.104798

Summary

Background **Asthenozoospermia is the primary cause of male infertility; however, its genetic aetiology remains poorly understood. Adenylate kinase 9 (*AK9*) is highly expressed in the testes of humans and mice and encodes a type of adenosine kinase that is functionally involved in cellular nucleotide homeostasis and energy metabolism. We aimed to assess whether *AK9* is involved in asthenozoospermia.**

Methods **One-hundred-and-sixty-five Chinese men with idiopathic asthenozoospermia were recruited. Whole-exome sequencing (WES) and Sanger sequencing were performed for genetic analyses. Papanicolaou staining, Haematoxylin and eosin staining, scanning electron microscopy, and transmission electron microscopy were used to observe the sperm morphology and structure. *Ak9*-knockout mice were generated using CRISPR-Cas9. Sperm adenosine was detected by liquid chromatography–mass spectrometry. Targeted sperm metabolomics was performed. Intracytoplasmic sperm injection (ICSI) was used to treat patients.**

Findings **We identified five patients harbouring bi-allelic *AK9* mutations. Spermatozoa from men harbouring bi-allelic *AK9* mutations have a decreased ability to sustain nucleotide homeostasis. Moreover, bi-allelic *AK9* mutations inhibit glycolysis in sperm. *Ak9*-knockout male mice also presented similar phenotypes of asthenozoospermia. Interestingly, ICSI was effective in bi-allelic *AK9* mutant patients in achieving good pregnancy outcomes.**

Interpretation **Defects in *AK9* induce asthenozoospermia with defects in nucleotide homeostasis and energy metabolism. This sterile phenotype could be rescued by ICSI.**

Abbreviations: AK9, Adenylate kinase 9; WES, Whole-exome sequencing; ATP, Adenosine triphosphate; GAPDS, Glyceraldehyde 3-phosphate dehydrogenase-S; LDHC, Lactate dehydrogenase C; AK, Adenylate kinases; ADP, Adenosine diphosphate; AMP, Adenosine monophosphate; MMAF, Multiple morphological abnormalities of the sperm flagella; PCD, Primary ciliary dyskinesia; OAT, Oligoasthenoteratozoospermia; WT, Wild-type; KO, Knockout; CRISPR-Cas9, Clustered regularly interspaced short palindromic repeats (CRISPR)/CRISPR-associated (Cas) endonuclease (Cas9); WHO, World Health Organization; SEM, Scanning electron microscopy; TEM, Transmission electron microscopy; FBS, Fetal bovine serum; DAPI, 4, 6-diamino-2-phenylindole; PBS, phosphate buffered saline; SCSA, Sperm chromatin structure assay; LC/MS, Liquid chromatography–mass spectrometry; ICSI, Intracytoplasmic sperm injection; GMP, Guanosine monophosphate; GDP, Guanosine diphosphate; GTP, Guanosine triphosphate; TCA, Tricarboxylic acid cycle; ExAC, Exome Aggregation Consortium; SIFT, Sorting Intolerant from Tolerant; PR, Progressive motility; NP, Non-progressive motility; NAG, N-acetyl-D-(+)-glucosamine; IF, Immunofluorescence; WB, Western blot; FSH, Follicle stimulating Hormone; LH, Lutenizing Hormone; PRL, Prolactin; E2, Estradiol; TZI, Teratozoospermia index; SDI, Sperm deformity index; DFI, DNA fragmentation index; HDS, High DNA stainability; MMP, Mitochondrial membrane potential

*Corresponding author.
**Corresponding author.
***Corresponding author.
E-mail addresses: linlithu@ccmu.edu.cn (L. Li), zhlpaper@fjmu.edu.cn (H. Zhou), qinwb@gdszjk.org.cn (W. Qin).
[h]These authors contributed equally to this work.

Funding The National Natural Science Foundation of China (82071697), Medical Innovation Project of Fujian Province (2020-CXB-051), open project of the NHC Key Laboratory of Male Reproduction and Genetics in Guangzhou (KF202004), Medical Research Foundation of Guangdong Province (A2021269), Guangdong Provincial Reproductive Science Institute Innovation Team grants (C-03), and Outstanding Young Talents Program of Capital Medical University (B2205).

Keywords: Asthenozoospermia; *AK9*; Nucleotide homeostasis; Energetic metabolism; Intracytoplasmic sperm injection

Research in context

Evidence before this study

Sperm motility is the outcome of the motion and beating of the flagella. Sufficient energy metabolism is indispensable for driving the movement of the sperm flagellum. However, the complex energy metabolic pathways that mediate sperm motility remain unclear.

Added value of this study

In the present study, we identified bi-allelic *AK9* mutations in infertile men with idiopathic asthenozoospermia. Spermatozoa from men harbouring bi-allelic *AK9* mutations decrease the ability of sperm to sustain nucleotide homeostasis. Noticeably, *Ak9*-knockout male mice also present similar phenotypes of asthenozoospermia. Intracytoplasmic sperm injection can effectively help patients with bi-allelic *AK9* mutations achieve good pregnancy outcomes.

Implications of all the available evidence

These findings demonstrate that defects in *AK9* induce asthenozoospermia with defects in nucleotide homeostasis and energetic metabolism; this sterile phenotype could be rescued by intracytoplasmic sperm injection.

Introduction

Approximately 15% of couples of childbearing age are affected by infertility, in which male-related factors account for nearly half of the cases.[1,2] Sperm motility is essential for sperm migration through the female reproductive tract and fertilisation.[3] Asthenozoospermia, characterised by reduced sperm motility, is generally considered a major factor contributing to male infertility.[4,5] Numerous studies have revealed the genetic contribution to asthenozoospermia, such as the *AKAP*, *TTC*, *DNAH*, and *CFAP* gene families.[6] However, the molecular pathogenesis of asthenozoospermia in most cases remains obscure, and its genetic aetiology is largely unknown.

The motility of spermatozoa is the outcome of the motion and beating of the flagella,[7] in which sufficient energy metabolism is indispensable for driving movement of mammalian sperm flagellum.[8,9] The energy from adenosine triphosphate (ATP) can be used directly by the spermatozoa, which is produced in the principal piece of the flagellum through glycolysis as well as in the mitochondria through oxidative phosphorylation.[10] Several pieces of evidence have indicated that some glycolytic enzymes are specifically expressed in the spermatozoa flagella, and that deletion of glycolytic genes, such as glyceraldehyde 3-phosphate dehydrogenase-S (*GAPDS*) or lactate dehydrogenase C (*LDHC*), profoundly inhibited sperm motility, leading to infertility and asthenozoospermia phenotype in male mice.[11,12] Oxidative phosphorylation, as a classical metabolic pathway, is also involved in energy metabolism in mouse sperm.[13] Sperm motility and ATP concentration were inhibited with mitochondrial respiratory inhibitors, and ablation of genes involved in mitochondrial respiration, such as deletion of testis-specific cytochrome c, could effectively decrease sperm motility and the rate of fertilisation *in vitro*, but cannot completely block fertilisation in mice.[14] However, scholars have observed that movement of mammalian sperm is not stopped immediately in the presence of glycolysis inhibitors, but remits motility for long periods.[15,16] Interestingly, both glycolysis and oxidative phosphorylation direct ATP generation via glucose oxidation; however, the motility of human spermatozoa can be sustained overnight in sugar-free medium, suggesting that, in addition to oxidative phosphorylation and glycolysis, other complex energy metabolisms are actively involved in regulating flagellar activity.[17,18] When ATP levels are low, adenylate kinases (AKs) can transfer phosphate groups to adenosine diphosphate (ADP), which in turn produces ATP for use in the mouse flagella.[19] Unfortunately, the complicated energy metabolism pathway that mediates sperm motility is not yet fully understood.

AKs are crucial regulators of intracellular nucleotide metabolic homeostasis, adenine nucleotide metabolism, and ATP regeneration and utilisation by catalysing the

reversible trans-phosphorylation reaction of two molecules of ADP to one molecule ATP and adenosine monophosphate (AMP) (2 ADP ⇌ ATP + AMP) in Plasmodium falciparum.[20] Considering the unique capability of AK to form β-ATP, AK-catalysed phosphotransfer doubles the energetic potential of ATP in failing hearts.[21] AKs have also been identified to be involved in energy generation and consumption in muscle and nerve cells.[22] Moreover, the dynamics of AK-catalysed phosphotransfer positively participate in cell and ciliary motility by integrating intracellular energy metabolism.[23] Remarkably, AK has been identified in the sea urchin sperm flagellum, which is essential for the flagellum mobility of sea urchin sperm.[24] It has also been demonstrated that flagellar AK effectively recovers the motility of detergent-inactive mouse sperm with the treatment of ADP, and sperm motility driven by ADP can completely propagate down the full flagellum, which presents more fluid waves than ATP alone.[19,25] CFAP45 links dynein ATPases to an axonemal module that converges on the AK pathway; a deficiency in *CFAP45* causes situs abnormalities and asthenospermia by disrupting an axonemal adenine nucleotide homeostasis module.[26] These previous studies highlight that *AK*s, as potentially functional regulators, contribute to sperm motility differently.

To date, nine *AK*s, namely *AK1–AK9*, have been identified.[27] *AK1* deficiency did not induce any defects in testis development, spermatogenesis, or sperm morphology and motility in mice under physiological conditions. However, in the detergent-modelled epididymal sperm with only ADP, *Ak1* disruption largely compromised sperm motility, which manifested as a smaller beating amplitude and higher beating frequency, resulting in less effective forward swimming.[28] AK1 and AK2 interact with soluble ODF4; the movement of the sperm flagella of *Odf4* knockout (KO) mice was affected owing to the loss of ODF4 with AK1 and AK2.[29] *SPOCD1* knockdown significantly inhibited cell proliferation and promoted apoptosis of human spermatogonial stem cells with downregulated *AK4*, and overexpression of *AK4* in *SPOCD1* knockdown cells partially reversed the phenotype.[30] Patrick Lorès reported that the c.2018T>G (p.Leu673Pro) transversion in *AK7* could cause severe asthenozoospermia in human beings due to multiple morphological abnormalities of the sperm flagella (MMAF) but not with primary ciliary dyskinesia (PCD) features.[31] Another team also independently identified a homozygous missense mutation (NM_152327: c.1846G>A; p.E616K) in *AK7* in two brothers with MMAF and oligoasthenoteratozoospermia (OAT) from a consanguineous family.[32] The protein encoded by *AK9*, also known as *AKD2*, contains multiple nucleotide-binding region domains and exhibits nucleoside monophosphate and diphosphate kinase activity that is essential for nucleotide homeostasis and energy metabolism.[33] Notably, *AK9* is highly expressed in the human testis and is involved in maintaining the homeostasis of cellular nucleotides by catalysing the interconversion of nucleoside phosphates.[33] However, because of the lack of selective AK inhibitors, the physiological effect of *AK9* in sperm and its role in the nucleotide homeostasis and energy metabolism has not been fully uncovered.

In this study, we recruited 165 infertile men with asthenozoospermia and identified bi-allelic *AK9* mutations in five patients from unrelated families. Spermatozoa from men harbouring bi-allelic *AK9* mutations have decreased potency to sustain nucleotide ratios, which significantly disrupts the regeneration of nucleotides and energy metabolism. Moreover, *Ak9* KO male mice presented with similar asthenozoospermia phenotypes. Taken together, these findings strongly suggest that *AK9* defects induce male infertility due to asthenozoospermia in humans and mice.

Methods

Human subjects

A cohort of 165 Chinese men with idiopathic asthenozoospermia was recruited at the Women and Children's Hospital of Xiamen University, as previously described.[34] The percentage of these patients' motile spermatozoa was lower than the reference value, with the progressive motility ranging from 0 to less than 32%. The other mean values of the semen parameters of the 165 patients are within the reference value range (in detail, pH ≥ 7.2, sperm count ≥39×10^6 spermatozoa per ejaculate, viability ≥58%, normal morphology of sperm ≥4%. Men with infertility exhibited normal external genitalia, bilateral testicular size, and hormone levels. Normal chromosomal karyotypes (46; XY) were identified in these 165 subjects, and no microdeletions were detected in the human Y chromosome, according to general protocols.[35,36] In addition, 200 healthy men with normal semen parameters who were fathers (one to four children) were recruited as control individuals.

Whole-exome sequencing and bioinformatic analysis

Whole-exome sequencing (WES) of the genomic DNA extracted from patients with asthenozoospermia was carried out as described previously.[37] Briefly, genomic DNA was extracted from peripheral blood samples using the DNeasy Blood and Tissue kit (Qiagen, Hilden, Germany), the human exome was enriched by SureSelect Human All Exon V6 (Agilent, California, USA), and then sequenced using the Illumina HiSeq Xten platform. The obtained data were aligned to the human reference sequence (hg19) using BWA 0.7.9a from the BWA-MEM algorithm. Picard software and Genome Analysis Toolkit were used to evaluate the quality of the variants. Selected candidate mutations were annotated in various databases. Variants satisfying the following

criteria were retained for subsequent analyses: absent or rare variants, nonsense variants, frameshifts, splice sites, and missense variants. Considering the patients' symptoms, testis-specific or highly expressed genes associated with the sperm structure or energy metabolism that met the screening criteria were prioritised. Sanger sequencing was used to authenticate these mutations. The primers used in this study are listed in Supplementary Table S1.

Protein structure prediction

The AK9 protein structure was predicted using the AlphaFold database. Wild-type (WT) and mutant AK9 protein structures were visualised and generated using UCSF Chimera (Version: 1.15, California, USA), as previously described.[38]

Construction of *Ak9* KO mice

Ak9 knockout mice were constructed using the Clustered Regularly Interspaced Short Palindromic Repeats (CRISPR)/CRISPR-associated (Cas) endonuclease (Cas9) (CRISPR-Cas9) genome-editing technology based on the C57BL/6 background, as previously described.[38] The sequence of guide RNAs was designed according to the online website https://zlab.bio/guide-design-resources; the gRNA sequence was 5′- GTTCCAGCTGCAGTCACTGT -3'. *Ak9* mutated F0 mice were mated with mice based on the C57BL/6 J background to generate homozygous offspring. All mice were housed under standard conditions at the Laboratory Animal Centre of Xiamen University.

Semen characteristics analysis

Semen characteristics analysis was performed according to the guidelines of the World Health Organization Laboratory Manual for the Examination and Processing of Human Semen (5th edition).[39,40] Human sperm samples were collected by masturbation into sterile cups after 2–4 days of sexual abstinence and were incubated in 5% CO_2 at 37 °C incubator for 30 min. Semen volume, sperm concentration, and sperm motility were evaluated using a computer-assisted sperm analysis (CASA) system (SCA SCOPE, Microptic, Barcelona, Spain), as described previously.[41,42] Sperm morphology was evaluated using Papanicolaou staining according to the World Health Organization (WHO) guidelines, as described previously.[43]

Electron microscopy analysis

Scanning electron microscopy (SEM) and transmission electron microscopy (TEM) analyses were performed as previously described.[38] For SEM analysis, both human and mouse sperm were fixed in 2.5% glutaraldehyde (Sigma–Aldrich, Missouri, USA), rinsed in 0.1 mol/L phosphate buffer, and treated with 0.5% Formvar. The slides were then dehydrated using an ethanol gradient and dried using a CO_2 critical-point dryer. After metal spraying with an ionic sprayer meter, the samples were observed using a Gemini SEM 500 (Zeiss, Baden-Württemberg, Germany). For TEM analysis, spermatozoa samples of the raw fraction were fixed with 2.5% glutaraldehyde (Sigma–Aldrich) for 3 h at room temperature (RT). After washing with phosphate buffer (0.1 M), the samples were immersed in 1% osmium tetroxide, dehydrated using graded ethanol concentrations, and infiltrated with acetone and SPI-Chem resin. After embedding in Epon 812, the ultrathin sections were stained with uranyl acetate and lead citrate. The ultrastructure of the spermatozoa was observed by TEM (JEM-1400, Jeol, Tokyo, Japan) at 60 kV.

Immunofluorescence

The immunofluorescence of the spermatozoa was performed as previously described.[38] The prepared spermatozoa were fixed in 4% paraformaldehyde for 30 min, and permeabilized with 0.2% Triton X-100 for 10 min. The sections were then blocked with 5% fetal bovine serum (FBS) for 60 min and incubated with primary antibodies overnight, followed by further staining with secondary antibodies for 60 min. After staining nuclei with 4, 6-diamino-2-phenylindole (DAPI; H-1200, Vector Laboratories, Burlingame, CA, USA), the fluorescence signal was acquired by confocal microscopy (Zeiss LSM 780; Zeiss, Ostalbkreis, Baden-Württemberg, Germany). These validated commercialised antibodies used for immunofluorescence are listed in Supplementary Table S2.

Western blotting

Western blotting was performed as previously described.[37] Briefly, proteins were separated on 10% SDS-PAGE and transferred to a polyvinylidene difluoride membrane (Immobilon-P PVDF membrane; Millipore, Bedford, Massachusetts, USA). Membranes were blocked for 1 h at room temperature with 5% skimmed milk in phosphate buffered saline (PBS). The membranes were incubated with specific primary antibodies at 4 °C overnight and then incubated with secondary antibodies for 1 h at room temperature. Detection was achieved using the ECL Plus Western Blotting substrate (Pierce, San Francisco, California, USA). Membranes were exposed to ChemiDoc MP Imaging System (Bio-rad, Hercules, California, USA). These validated commercialised antibodies are listed in Supplementary Table S2.

Haematoxylin and eosin staining

Mouse testes were fixed in 4% paraformaldehyde at 4 °C overnight and rinsed in 0.1 mol/L phosphate buffer for 10 min. Next, the testicles were progressively dehydrated using an ethanol gradient, penetrated with xylene, and embedded in paraffin. Sections 5 μm-thick were mounted on slides coated with L-lysine followed by deparaffinisation and rehydration. For haematoxylin and

eosin (HE) staining, the slides were stained with haematoxylin (ZLI-9610, ZSbio, Beijing, China) and eosin (ZLI-9613, ZSbio), as described previously.[44]

Sperm DNA fragmentation detection and sperm DNA stainability

A small fraction of each human semen sample was taken (Raw fraction) for sperm chromatin structure assay (SCSA), as described elsewhere.[45] In brief, 200 µl TNE buffer was added to the appropriate amount of semen to attain an approximate $1–2 \times 10^6$ sperm/ml and add 400 µl of acid detergent solution. Then, 1.20 ml Acridine Orange (AO) staining solution was added and mixed by vortexing. The samples were then analysed using flow cytometry (BD FACSCanto, BD Biosciences, San Jose, USA).

Detection of sperm adenosines

The prepared sperm samples were suspended in an extraction solution (methyl alcohol: H_2O = 7:3) and freeze-thawed three times with liquid nitrogen. The sample was then vortexed for 5 min and centrifuged at 13,000 rpm for 15 min at 4 °C, and the supernatants were removed to 2 mL tubes and lyophilised by a concentrator (Labconco corporation, Kansas, USA). Finally, the concentrates were resolved with 50% acetonitrile–water containing 0.03% formic acid and subjected to liquid chromatography–mass spectrometry (LC/MS) (AB SCIEX QTRAP 5500). The standard substances were obtained from Shanghai Yuanye Biotechnology Co., LTD (Yuanye, Shanghai, China).

Phosphotransfer rates

AK-catalysed phosphotransfer in sperm was measured using the [^{18}O] phosphoryl labelling technique. Briefly, sperms were collected, washed in 0.9 NaCl, and centrifuged at 300×*g* for 5 min. Then, the sperm were incubated in a TYH (Toyoda, Yokoyama, Hoshi, Japan) medium containing 10% [^{18}O] water for 30 s at 37 °C in 5% CO_2 followed by centrifuging at 500×*g* for 5 min to collect the sperm. The sperm deposits were added to the nucleoside extraction solution and freeze-thawed three times with liquid nitrogen. The sample was then vortexed for 5 min and centrifuged at 13,000 rpm for 15 min at 4 °C. The supernatants were transferred into 2 mL tubes and lyophilised using a low-temperature vacuum centrifugal concentrator (Labconco Corporation, Kansas, USA). Finally, the concentrates were resolved with 50% acetonitrile–water containing 0.03% formic acid and loaded onto an LC/MS (QTRAP 5500, SCIEX, Framingham, USA). β-ATP was recorded to evaluate AK-catalysed phosphotransfer.

Mitochondrial membrane potential detection

The sperm were collected, washed in 0.9% NaCl, and centrifuged at 300×*g* for 5 min. The suspensions were removed, and the sperm sediments were incubated in TYH (Toyoda, Yokoyama, Hoshi, Japan) medium at 37 °C in 5% CO_2. Next, the samples were stained with JC-1 for 15 min at 37 °C according to instructions of the mitochondrial membrane potential (MMP) assay kit (C2006, Beyotime, Shanghai, China). The MMP was detected using flow cytometry (BD FACSCanto, BD Biosciences, San Jose, CA, USA).

Targeted sperm metabolomics analysis

Targeted sperm metabolomics analysis based on the multiple reaction monitoring (MRM) approach was performed by Shanghai Applied Protein Technology Co., Ltd. Briefly, the sperm samples were preconditioned with ultrapure water for homogenisation. Then, 800 µl pre-cooled methanol/acetonitrile (1:1, v/v) was added and the mixture was sonicated in the ice bath for 20 min, followed by incubation at –20 °C for precipitation of proteins. The samples were subsequently centrifuged for 20 min at 4 °C and the supernatants were collected. Finally, the supernatants were analysed on an Agilent 1290 Infinity LC system coupled with an AB 5500 QTRAP mass spectrometer (SCIEX, Framingham, MA, USA) in the negative ion mode, followed by the identification and quantification of targeted metabolites.

Label-free quantitative proteomic analyses

Label-free quantitative proteomic analyses were performed as described previously.[46] Germ cells were lysed in SDT buffer and proteins were quantified using a BCA Protein Assay Kit. Each sample was processed using a filter-aided proteomic preparation method. Peptides were desalted using a C18 cartridge and re-suspended in 0.1% formic acid. Samples were analysed by LC-MS/MS using an Easy nLC system (Thermo Fisher, Waltham, USA). Buffer A was an aqueous solution of 0.1% formic acid and buffer B was a solution of acetonitrile in 0.1% formic acid. Trapping was performed on a NanoViper C18 column (Acclaim PepMap100, Thermo Fisher, Waltham, USA). Elution was performed using a Thermo Scientific C18-A2 EASY column. Analytical separation of the peptides was achieved at a flow rate of 300 nL/min using a Orbitrap Exploris 480 mass spectrometer. The dynamic exclusion time window was set to 60 s. The data were acquired using a normalised collision energy of 30 eV. Quantitative analysis was performed using MaxQuant software (version 1.5.3.17; Max Planck Institute of Biochemistry, Germany).

Intracytoplasmic sperm injection

The intracytoplasmic sperm injection (ICSI) procedure used by the patients in this research was consistent with a previous report.[47,48] In brief, in the female partners, ovulation was triggered by the combined administration of a gonadotropin-releasing hormone agonist (GnRH-a; Enantone, Takeda Osaka Plant, Osaka, Japan), recombinant follicle stimulating hormone (r-FSH; Gonal-F,

Serono Laboratory Co. Ltd., Geneva, Switzerland), highly purified menotrophin (HP-HMG; Menopur, Ferring International Center SA, Kiel, Germany), and 250 μg recombinant human chorionic gonadotropin (r-HCG; Ovidrel, Serono Laboratory Co. Ltd., Japan). GnRH-a was administered at 3.75 mg on day 4 of menstruation, followed by 1.875 mg 28 days later. r-FSH and HP-HMG were administered daily until the dominant follicles reached 3 and a mean diameter reached 18 mm, after which rHCG was administered to induce ovulation. Vaginal ultrasound-guided follicular puncture was performed 36 h after r-HCG injection and mature oocytes were retrieved.[49,50] Male patients ejaculated after masturbation on the day of oocyte retrieval. The semen was centrifuged at 1400 rpm for 10 min, and the sperm pellet was re-suspended in 150 μL of medium for ICSI. The embryos were grown in Vitrolife G-SERIES culture media (Vitrolife, Goteborg, Sweden). The fertilisation rate was calculated after performing ICSI for 18 h.[51–53] Three days after ICSI, the embryos were transferred into the uterus of the female partner, who were prescribed 200 mg oral progesterone (Utrogestan; Laboratories Besins International, Montrouge, France) twice daily for 12 days and 90 mg topical 8% progesterone daily (Crinone; Fleet Laboratories Limited, Watford, England). Clinical pregnancy was established using ultrasonography at 6 weeks of gestation, and the clinical outcome was evaluated by the delivery of a healthy baby.

Ethics

This study was approved by the Ethics Committee of Women and Children's Hospital of Xiamen University (KY-2019-060). Informed consent was obtained from all enrolled participants prior to their participation. All the research involving human research participants was performed in accordance with the Declaration of Helsinki. Experiments on mice were approved by the Animal Welfare Committee of the Research Organization of Xiamen University (XMULAC20200143) and were conducted in accordance with the guidelines of the Laboratory Animal Centre of Xiamen University on Animal Care.

Role of the funding source

The funders played no role in the study design, data collection, data analyses, interpretation, or writing of the manuscript.

Results

Identification of bi-allelic *AK9* mutations in men with asthenozoospermia

To investigate the potential genes associated with male asthenozoospermia, we recruited 165 infertile men with idiopathic asthenozoospermia and performed WES and bioinformatic analyses. We identified bi-allelic mutations in *AK9* (MIM:615358) in five sporadic individuals, two of whom came from unrelated consanguineous families and harboured homozygous mutations (Table 1).

In the patient F013/II-I who came from a consanguineous family, a homozygous frameshift insertion mutation, NC_000006.11:g.109820419_109820422dup *AK9* was identified and confirmed (Fig. 1a). Another homozygous frameshift insertion mutation, NC_000006.11:g.109906435dup in *AK9* was identified in the patient R0008/II-1 (Fig. 1b). We identified a compound heterozygous non-frameshift deletion mutation NC_000006.11:g.109980462_109980470del and a stop-loss mutation NC_000006.11:g.109954114T>A of *AK9* in the R0022/II-1, which was confirmed by Sanger sequencing (Fig. 1c). Similarly, compound heterozygous mutations NC_000006.11:g.109885474G>A and NC_000006.11:g.109854633C>T were identified and confirmed in the R0038/II-1 (Fig. 1d), and compound heterozygous mutations NC_000006.11:g.109819141C>T and NC_000006.11:g.109863352_109863354del were identified and confirmed in the R0052/II-1 (Fig. 1e). Sanger sequencing was also performed on the parents, and the results confirmed that they were heterozygous carriers (Fig. 1). The transcript of *AK9* (ENST00000424296.7) was 6326 bp and encoded 41 exons. As indicated by red arrows, all eight mutation sites were located in the exons of the *AK9* transcript (Fig. 1f). Therefore, patients with asthenozoospermia are likely to have genetic defects in *AK9*, which is inherited from their parental heterozygous carriers and followed autosomal recessive inheritance in a Mendelian pattern.

In silico analysis of the bi-allelic *AK9* mutations

The transcript of human *AK9* (UniProtKB, Q5TCS8) was predicted to generate a protein with three AK domains, three NMP-binding domains, and three LID domains. The p.Glu203_Glu205del mutation-affected amino acids are located in the AK1 domain. p.Glu1086del and p.Glu1131Lys mutation-affected amino acids were located in the AK2 domain. The amino acids affected by the p.Ter422Tyrext*27, p.Cys669Leufs*4, and p.Pro815Leu mutations are located between AK1 and AK2 domains. The p.Cys1626Valfs*16 and p.Val1692Met mutations impact the C-terminus of AK9 (Fig. 2a).

We constructed a three-dimensional structure of AK9 using UCSF Chimera with AlphaFoldDB (AF-Q5TCS8-F1) predicted by AlphaFold to visually show the effects of these mutations on the AK9 protein. Compared to the WT AK9 protein (Fig. 2b), the early termination of protein translation caused by the p.Cys1626Valfs*16 frameshift insertion in F013/II-1 (Fig. 2c), and p.Cys669Leufs*4 frameshift insertion in R0008/II-1 (Fig. 2d) significantly affected the three-dimensional structure of the protein. The p.Glu203_Glu205del mutation caused a deletion of three amino acids and the p.Ter422Tyrext*27 stop-loss mutation resulted in a 27

amino acid extension of R0022/II-1 (Fig. 2e). The compound heterozygous p.Glu1131Lys and p.Pro815Leu mutations induced significant changes in the amino acid side-chains of R0038/II-1 (Fig. 2f). The p.Val1692Met mutation also induced a significant change in the amino acid side chain, and p.Glu1086del caused the 1086th amino acid deletion in R0052/II-1 (Fig. 2g).

In silico analysis demonstrated that these mutations were absent or rare in the human genome datasets archived in the ExAC, 1000 Genomes Project, gnomAD _exome (All), and GnomAD _exome (East Asian) databases (Table 1). In addition, the amino acid residues affected by *AK9* mutations were predicted to be conserved in PhyloP and PhastCons (Table 1). Moreover, we aligned the amino acid sequences of AK9 across different species and found the amino acids affected by the mutations were all highly conserved from *Homo sapiens* to *Ictalurus punctatus*, which suggests that these sites affected by the identified mutations may play an essential role in the long-term evolutionary history (Supplementary Fig. S1). In addition, these mutations were found to be potentially deleterious using SIFT, PolyPhen-2, and MutationTaster tools (Table 1).

Asthenozoospermic phenotype in men harbouring bi-allelic *AK9* mutations

Clinical examinations were performed for primary male infertility associated with bi-allelic *AK9* mutations. These patients showed normal physical development, normal development of the organs and accessory glands of the reproductive system, and normal serum hormone levels (Supplementary Table S3). No obvious abnormalities were observed on paranasal sinus CT images (Supplementary Fig. S2a), chest CT images (Supplementary Fig. S2b), and chest radiographs (Supplementary Fig. S2c) between with *AK9*-mutated patients and controls. Analysis of sperm parameters showed that the volume and concentration were within the normal ranges (Table 2); however, sperm motility and progressive motility were significantly lower than the reference limits in *AK9*-mutated patients (Table 2).

Morphological and structural characteristics of spermatozoa from *AK9* mutant patients

It is worth noting that the percentage of normal morphological spermatozoa, teratozoospermia index (TZI), and sperm deformity index (SDI) did not show any abnormalities in sperm from patients with bi-allelic *AK9* mutations, according to the WHO reference values (Supplementary Table S4). The DNA fragmentation index (DFI) and high DNA stainability (HDS) values were within the reference range (Supplementary Table S4).

Papanicolaou staining indicated that the head and flagella of sperm from patients with bi-allelic *AK9* mutations were in accordance with those of control subjects (Fig. 3a), which was further confirmed by the SEM results (Fig. 3b). Moreover, TEM was employed to

	Subject									
	F013 II-1		R0008 II-1		R0022 II-1		R0038 II-1		R0052 II-1	
Gene	AK9		AK9		AK9		AK9		AK9	
cDNA alteration	c.4872_4875dupGTTA		c.2005dupT		c.607_615del	c.1266 A>T	c.3391G>A	c.2444C>T	c.5074G>A	c.3257_3259del
Protein alteration	p.Cys1626Valfs*16		p.Cys669Leufs*4		p.Glu203_Glu205del	p.Ter422Tyrext*27	p.Glu1131Lys	p.Pro815Leu	p.Val1692Met	p.Glu1086del
Variant type	frameshift insertion		frameshift insertion		nonframeshift deletion	stoploss	nonsynonymous SNV	nonsynonymous SNV	nonframeshift deletion	nonsynonymous SNV
Allele frequency in human populations										
ExAC	0		0		0.0002	0.0002	0.00003319	0	0.00002946	0.00002946
1000 Genomes Project	0		0		0	0	0.00199681	0	0	0
gnomAD _exome (All)	0.00000459		0		0.000178	0.0001	0.00003726	0.000006864	0.0000438	0.0000378
GnomAD _exome (East Asian)	0.0000623		0		0.000604	0.00006347	0.0005	0.0000985	0.0000544	0.000169
Conservation of the affected amino acid residues										
PhyloP	6.805		−2.434		−0.346	−1.682	5.504	6.634	3.125	1.343
PhastCons	1.000		0.001		0.870	0	0.998	1	1.000	1.000
Functional prediction										
SIFT	N/A		N/A		N/A	N/A	Damaging	Damaging	Damaging	N/A
PolyPhen-2	N/A		N/A		N/A	N/A	Probably_damaging	Probably_damaging	Probably_damaging	N/A
MutationTaster	N/A		N/A		N/A	Polymorphism	Disease_causing	Disease_causing	Disease_causing	N/A

AK9, adenylate kinase 9; ExAC, Exome Aggregation Consortium; SIFT, Sorting Intolerant from Tolerant; N/A, not applicable.

Table 1: **Bi-allelic *AK9* variants identified in Chinese men with asthenozoospermia.**

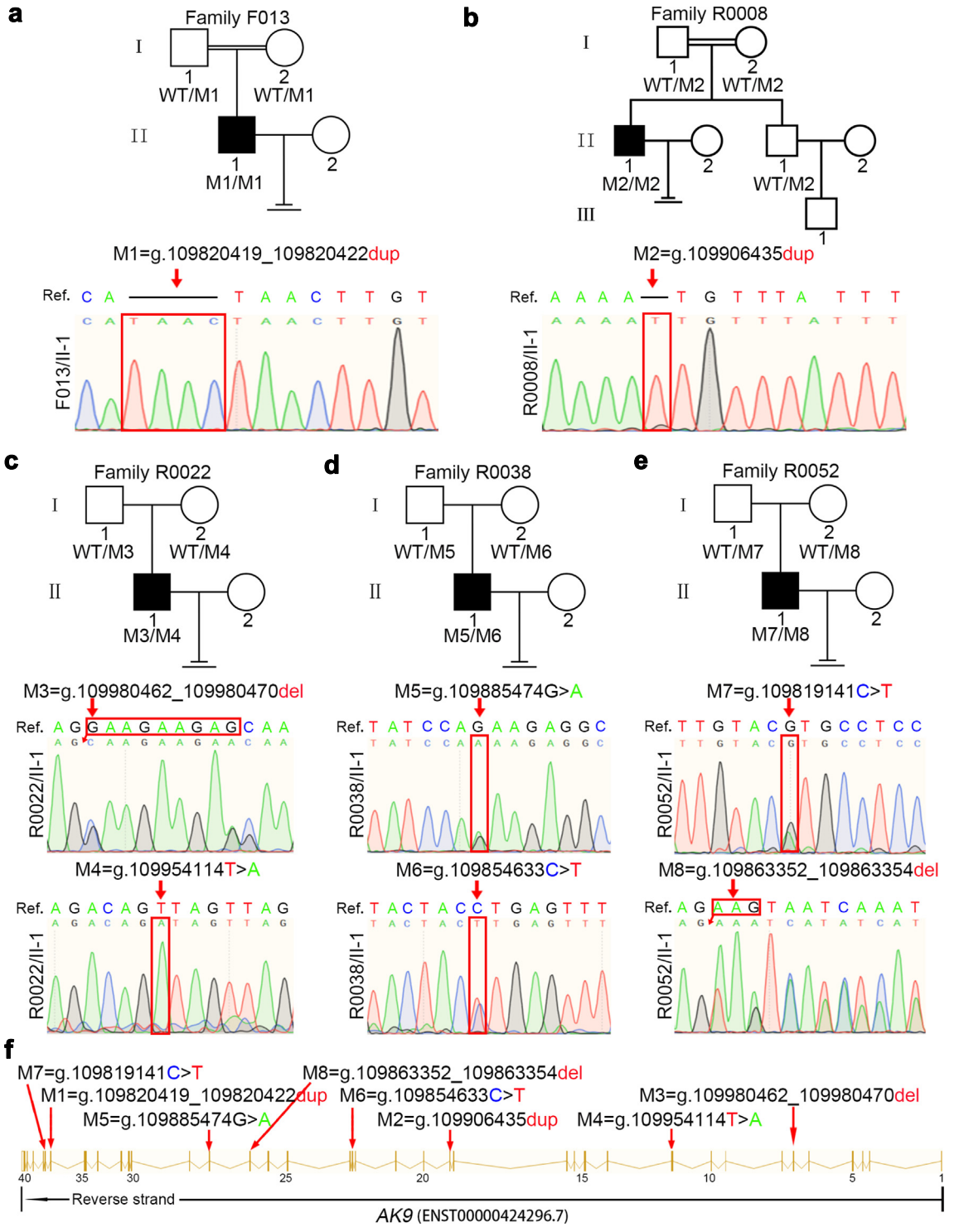

Fig. 1: Pedigree-based identification of the bi-allelic *AK9* mutations from five infertile patients with asthenozoospermia. **(a–e)** Pedigree chart of the five patients with asthenozoospermia affected by bi-allelic *AK9* mutations. The black squares represent the affected individuals. Sanger sequencing results are shown below the pedigrees. The mutation positions are indicated by red arrows or red rectangles. **(f)** The location of the mutated base sites on the genome of *AK9*.

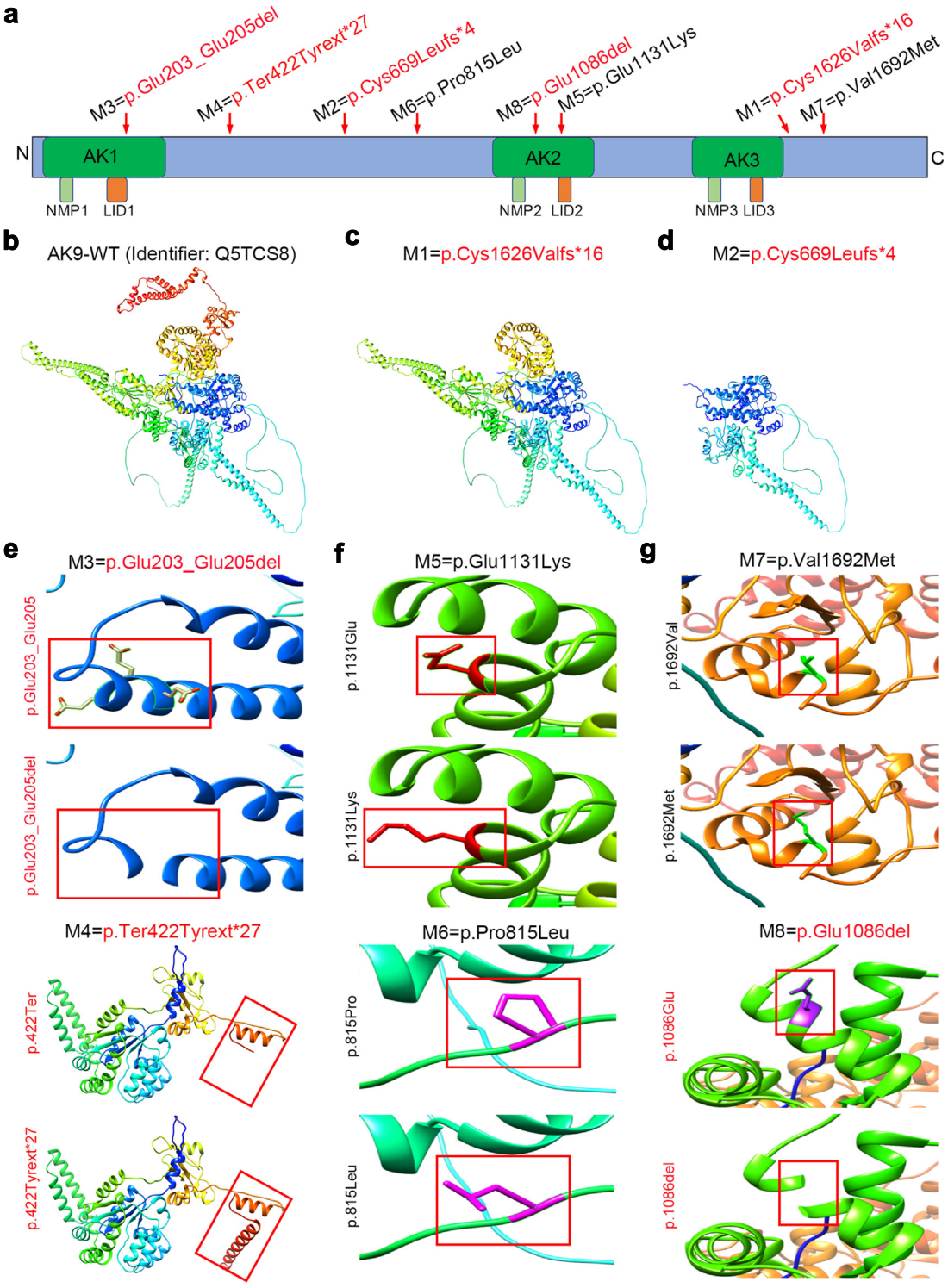

Fig. 2: Effect of mutant sites on the structure of the AK9 protein. **(a)** The position of the amino acid substitutions on the secondary structure of AK9. The dark green rectangles represent the "adenylate kinase" domain, the light green rectangles represent the "NMPbind" domain, and the orange rectangles represent the "LID" domain. **(b)** The three-dimensional structure of wild-type (WT) AK9 (AlphaFoldDB: AF-Q5TCS8-F1) protein. **(c–d)** Three-dimensional structure of AK9 residues after homozygous frameshift insertion mutations. **(e–g)** Local magnification of changes in amino acid residues between the WT and mutated AK9 protein in compound heterozygous patients.

	F013 II-1	R0008 II-1	R0022 II-1	R0038 II-1	R0052 II-1	Reference
Volume (ml)	2.2–3.5	3.8–4.5	2.5–3.2	2.6–3.2	2.5–3.8	≥1.5 ml
Concentration (10^6/ml)	19.6–34.4	22.2–54.2	28.6–78.5	25.76–56.36	18.65–40.24	≥15 × 10^6/ml
Progressive motility (%)	0.6–3.5	0.5–2.9	1.5–3.8	1.2–2.6	2.6–5.6	≥32%
Non-progressive motility (%)	4.5–10.9	5.3–13.9	6.2–12.3	3.6–14.2	5.6–10.3	–
Total activity (PR + NP) (%)	3.6–12.6	5.8–16.8	7.7–16.1	4.8–16.8	8.2–15.9	≥40%
Vitality (%)	32	22	29	26	24	≤40%
Normal flagella (%)	45	58	63	57	65	>23.0
Absent flagella (%)	4	3	4	5	3	<5.0
Short flagella (%)	5	2	1	3	2	<1.0
Coiled flagella (%)	14	16	9	11	8	<17.0
Angulation (%)	13	9	5	8	11	<13.0
Irregular caliber (%)	3	2	4	1	5	<2.0
NAG (mU)	65.38	107.67	112.86	110.45	85.41	≥20mU/per ejaculation
Fructose (umol)	17.32	15.27	20.18	18.56	21.76	≥13μmol/per ejaculation
Zinc (umol)	2.85	4.1	5.63	4.86	3.65	≥2.4μmol/per ejaculation

PR, Progressive motility; NP, Non-progressive motility; NAG, N-acetyl-D-(+)-glucosamine. Lower and upper reference limits are shown according to the World Health Organization standards and the distribution ranges of morphologically abnormal spermatozoa observed in fertile individuals.[54,55]

Table 2: **Semen characteristics and sperm motility in men with bi-allelic *AK9* mutations.**

investigate deficiencies in the axoneme ultrastructure of the spermatozoa from these patients. We observed that the sperm ultrastructure at the mid-piece of the flagella was indistinguishable in appearance between the normal control and *AK9* defect patients (Fig. 3c). However, although AK9 is mainly expressed in the sperm flagellum of control subject, it was absent in the sperm flagellum of the patients (Fig. 3d).

Bi-allelic *AK9* mutations affect the homeostasis of sperm nucleotides

The AK9 protein is a nucleoside monophosphate and diphosphate kinase that is highly expressed in the testes. Therefore, we performed targeted metabolomic analysis to investigate the components of the nucleotide metabolic process in patient F013/II-1. As expected, ATP levels in the patient's sperm were significantly diminished (Fig. 4a). Compared with control nucleoside levels, sperm from *AK9*-deficient patients showed significantly decreased AMP and ADP levels. The levels of guanosine monophosphate (GMP), guanosine diphosphate (GDP), and guanosine triphosphate (GTP) were also decreased (Fig. 4a). Therefore, the sperm in the *AK9*-deficient patient displayed lower levels of nucleotides than that in the control subject.

AK9 defect disrupts the flow of energy metabolism in sperm

AK-catalysed phosphotransfer, a hub within the metabolic regulatory system, is frequently coupled with cellular bioenergetic networks, including oxidative phosphorylation and glycolysis. We measured the sperm MMP of the patients using JC-1 staining; the spermatozoa from *AK9*-mutated patients showed no significant deficiency in the MMP compared with the normal levels (Supplementary Table S4). Oxidative phosphorylation was further assessed by monitoring the levels of tricarboxylic acid cycle (TCA) metabolites; the TCA-related metabolites of the spermatozoa from patient F013/II-1 were comparable to those in the control individual (Supplementary Fig. S3). Glycolysis was then evaluated by monitoring the levels of the metabolites; glycolysis-related metabolites in the spermatozoa from patient F013/II-1 were significantly decreased compared with those in the control individuals (Fig. 4b). These diminished levels of glycolytic intermediates indicated that the defect in *AK9* reduced glycolytic metabolism in the patient's sperm.

Due to the unique role of AK in-phosphotransfer, we evaluated the phosphoryl moiety in ATP. Surprisingly, ^{18}O-labelled-ATP was significantly reduced, indicating insufficient AK-catalysed phosphotransfer in the sperm of patients with *AK9* deficiency (Fig. 4c). These results suggest that bi-allelic mutations in *AK9* disrupt glycolytic metabolic homeostasis and inhibit AK-catalysed phosphotransfer in human sperm.

MS of sperm proteins from *AK9*-deficient patients

We performed label-free quantitative proteomics of sperm from control subjects and the *AK9* mutated patient F013/II-1. The results showed that the levels of approximately 211 proteins were increased and the levels of 195 proteins were decreased by more than 1.5-fold (Supplementary Table S5). The differentially expressed proteins in the spermatozoa from the *AK9*-mutated patient compared to control subjects are shown in a heat map (Fig. 4d). Gene ontology analysis showed that the downregulated proteins (Fig. 4e) or upregulated proteins (Fig. 4f) were enriched in carbohydrate

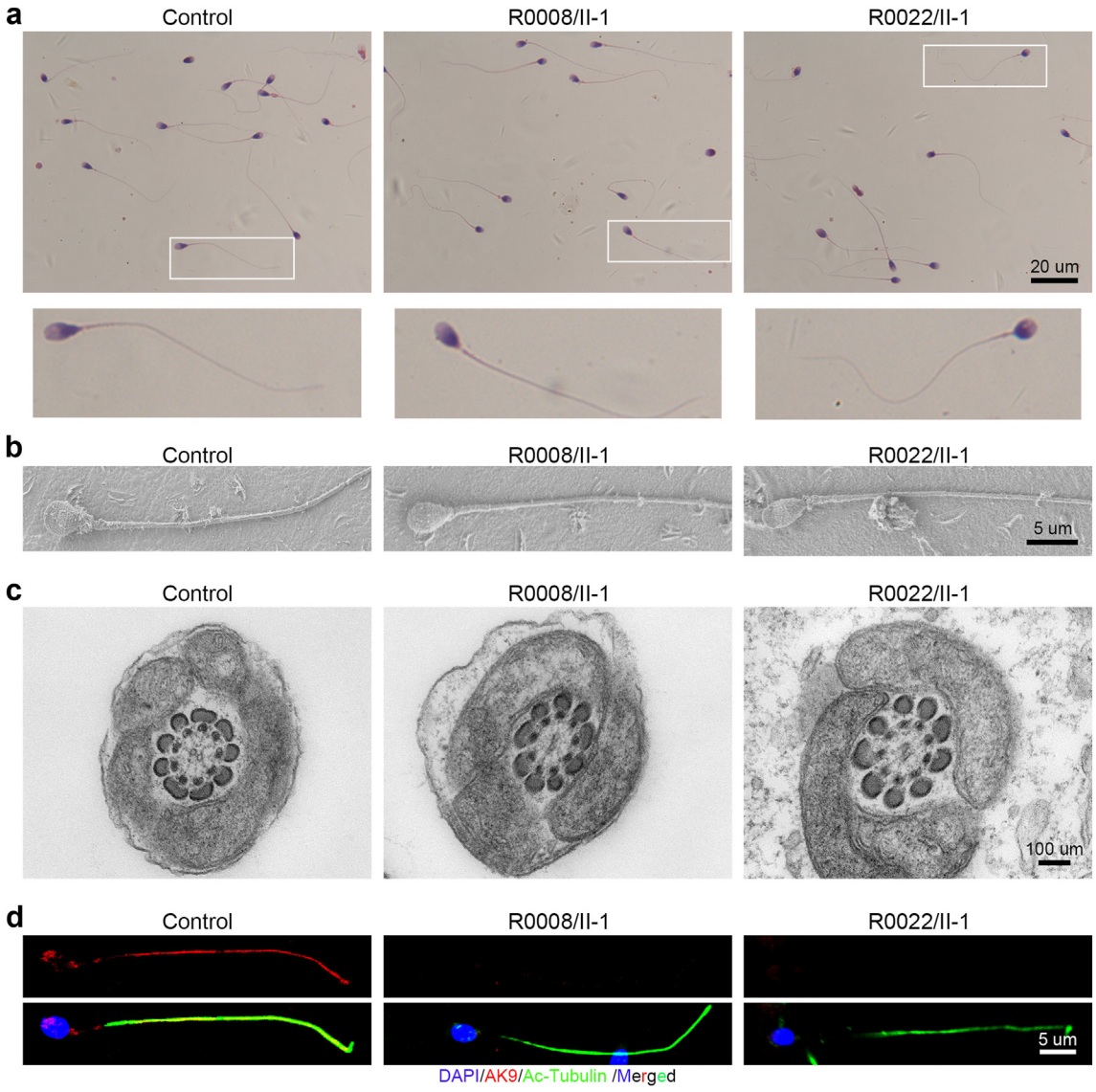

Fig. 3: Morphology and ultrastructure of the spermatozoa from patients affected by bi-allelic *AK9* mutations. **(a)** Morphological analysis of the spermatozoa from a control subject and the patients with bi-allelic *AK9* mutations. Scale bar: 20 μm. **(b)** Field emission-scanning electron microscopy (FE-SEM) analysis of the morphological characteristics of the patients' spermatozoa. Scale bar: 5 μm. **(c)** Ultrastructural analysis of the spermatozoa flagella from the patients at the mid-piece. Scale bar: 100 μm. **(d)** Immunofluorescence analysis of AK9 expression in the patients' spermatozoa flagella. Scale bar: 20 μm.

transport and metabolism, energy production and conversion, nucleotide transport and metabolism, signal transduction mechanisms, secondary metabolite biosynthesis, transport, and catabolism (Fig. 4g).

Ak9 KO male mice resemble asthenozoospermic phenotypes

To determine the expression of *Ak9* in various mouse tissues, we performed qRT-PCR for *Ak9* mRNA. The results showed that *Ak9* mRNA was highly expressed in the testes (Supplementary Fig. S4a). To further confirm the role of *Ak9* in sperm motility, we constructed *Ak9*-null mice using CRISPR-Cas9 technology (Supplementary Fig. S4b). Sequencing results showed that 82 bp bases were deleted in the *Ak9* exon (Supplementary Fig. S4c), and Western blotting confirmed the absence of AK9 in the testes of KO mice (Supplementary Fig. S4d). The immunofluorescence results further confirmed that AK9 was absent in the flagellum of KO mice and that AK9 was mainly expressed in the sperm flagellum of WT mice (Supplementary Fig. S4e).

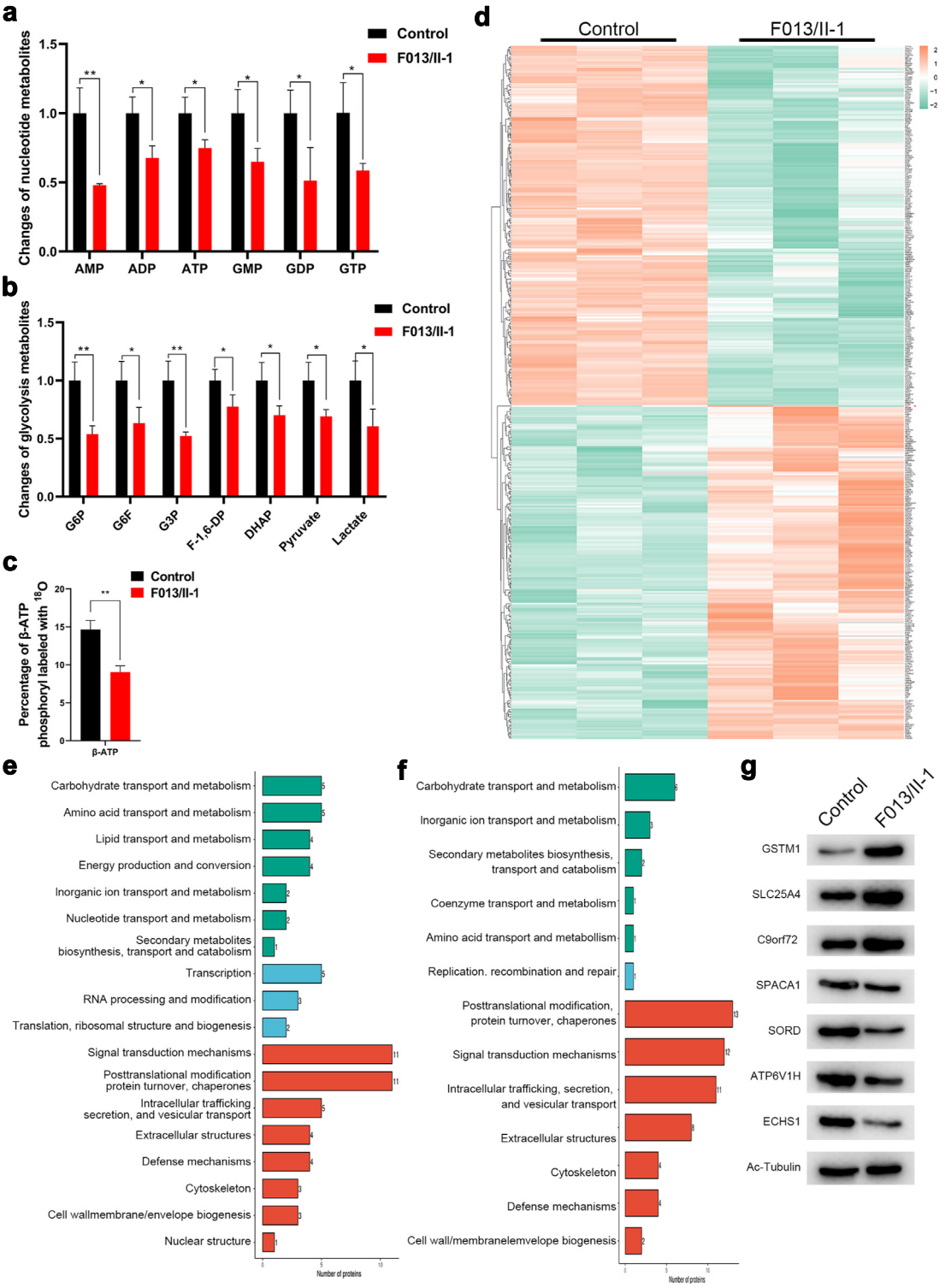

Fig. 4: Metabolite analysis of the spermatozoa from the patient F013/II-1 affected by a bi-allelic *AK9* mutation. **(a)** Changes in the nucleotide metabolites in the spermatozoa from the *AK9* mutated patient F013/II-1 compared with the control subjects (*p < 0.05, **p < 0.01). **(b)** Changes in the glycolytic metabolites in the spermatozoa from the *AK9* mutated patient F013/II-1 compared with the control subjects. **(c)** The percentages of β-ATP phosphoryl labelled with ^{18}O in the spermatozoa from the *AK9* mutated patient F013/II-1 compared with the control

The *Ak9*-deficient male mice survived and did not display any significantly developmental abnormalities. We performed SEM and TEM for the trachea and lung of the *Ak9* KO mice and the results showed no significant defects in the cilia of the trachea (Supplementary Fig. S5a) and lung (Supplementary Fig. S5b). Moreover, the appearance of the testes and epididymis were generally similar between *Ak9*-null and WT male mice (Supplementary Fig. S6a). Compared to the controls, the weight of the body (Supplementary Fig. S6b), testes (Supplementary Fig. S6c), and epididymis (Supplementary Fig. S6d) of *Ak9*-null male mice were not significantly different. HE staining indicated that spermatozoa were produced in the testes of *Ak9*-null mice (Supplementary Fig. S6e), and the number of spermatozoa in the epididymis was not significantly different from that in control mice (Supplementary Fig. S6f).

Papanicolaou staining showed that sperm from *Ak9*-null mice exhibited normal morphology (Fig. 5a). Consistent with the patients' sperm, the results of the TEM analysis showed no obvious defects in the ultrastructure of the flagella from *Ak9*-null mice at the midpiece (Fig. 5b) or principal piece (Fig. 5c).

The percentage of motile sperm in *Ak9*-null mice was significantly lower than that in WT mice (Fig. 5d), suggesting that *Ak9* ablation impaired sperm mobility. We also detected disordered adenosine metabolism and a marked decrease in AMP, ADP, ATP, GMP, GDP, and GTP levels in epididymal sperm from *Ak9* KO mice compared with those from WT mice (Fig. 5e). Moreover, the ablation of *Ak9* decreased glycolytic metabolism (Fig. 5f) and β-phosphoryl ATP production (Fig. 5g). Collectively, these results further confirm that *AK9* deficiency impairs male fertility due to asthenozoospermia in humans.

AK9-associated male infertility could be rescued by ICSI in humans and mice

Accumulating evidence has shown that ICSI with ejaculated sperm is effective in most cases of asthenozoospermia. In this study, we performed ICSI using epididymal sperm from *Ak9* KO mice and assessed that the 2 PN rate (% of 2PN/total) and birth rate (% of live offspring/transferred embryos) of the *Ak9* knockout mice comparable than those of WT mice (Fig. 5h).

ICSI was performed on subjects F013/II-1, R0008/II-1, and R0022/II-1. Day-3 high-quality cleavage embryos (Fig. 6) were transferred under ultrasound guidance. In all three cases, a healthy pregnancy was issued with the delivery of healthy babies (Table 3).

Discussion

Sperm motility is essential for male reproduction and is only achieved when dynamic ATP effectively supports it.[56] Glycolysis and oxidative phosphorylation are positively involved in the support of energy by catabolising glucose to generate ATP in mammalian sperm.[57] However, mammalian sperm motility lasts for quite a long time in glucose-free medium.[18,58] Thus, the energy metabolism of sperm is not yet fully understood.

AKs have been identified in prokaryotes and eukaryotes and play an important role in maintaining nucleotide and energy homeostasis in cells by interconverting stoichiometric amounts of ATP and AMP with two ADP molecules.[59–62] AKs are abundant in tissues and cells with a high energy demand, such as the heart, skeletal muscle, and sperm, in mice.[63,64] AK-catalysed phosphotransfer not only provides an additional energetic source, but also doubles the utilisation of ATP. Sperm motility is reactivated in the presence of ADP alone in mice and bovines, but these motile sperm are immediately stopped by P1, P5-di (adenosine 5′)-pentaphosphate (Ap5A), an AK-specific inhibitor.[25,65] AK-catalysed phosphotransfer is essential for sperm motility in sea-urchins.[18,24,66] Thus, AKs play an important role in flagellar motility.

We identified two patients harbouring homozygous mutations and three patients carrying compound *AK9* mutations among 165 sterile men with asthenozoospermia using WES analysis. AK9, a nucleoside mono- and diphosphate kinase, plays important roles in nucleotide homeostasis and ATP regeneration and utilisation by catalysing the interconversion of adenine nucleotides, and is preferentially expressed in the testes of humans and mice. These mutated sites are rare or absent in humans, and the amino acid residues affected by these mutations are conserved in many species, suggesting that *AK9* deficiency may be a primary cause of asthenozoospermia in humans.

Sperm motility depends on energy metabolism. Destruction of oxidative phosphorylation and glycolysis prevents sperm motility and induces asthenozoospermia by inhibiting ATP generation.[67] Remarkably, AKs can salvage energy by converting ADP to ATP, and the functions of AKs have been reported in excitation–contraction coupling, nuclear transport, the energetics of the cell cycle, as well as cell and ciliary motility.[23] In the sperm of mice, ADP alone effectively reactivates motility, and ADP-reactivated sperm exhibited a higher amplitude, suggesting AKs are involved in sperm motility and are a key modulator of the waveform.[25] Our

subjects. **(d)** Heat map of differentially expressed proteins in the spermatozoa from the *AK9* mutated patient F013/II-1 compared with the control subjects. Orange represents high expression, and green represents low expression. **(e)** Signalling pathways involved in the down-regulated expression of proteins in the spermatozoa from the *AK9* mutated patient F013/II-1 compared with the control subjects. **(f)** Signalling pathways involved in the upregulated expression of proteins in the spermatozoa from *AK9* mutated patient F013/II-1 compared with the control subjects. **(g)** Western blot confirmed the protein levels of proteomics analyses.

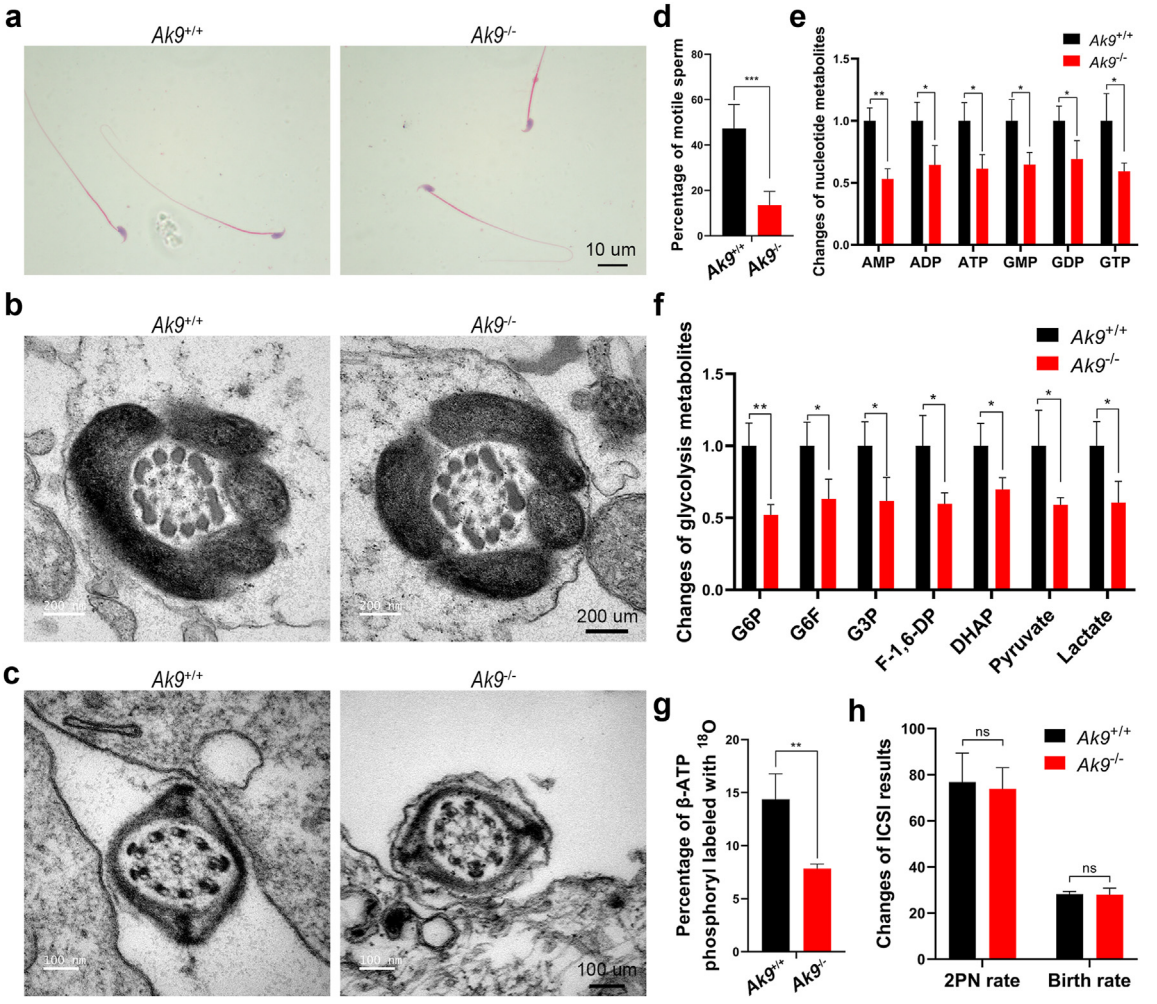

Fig. 5: The phenotype of the *Ak9* knockout mice. **(a)** Morphological analysis of the sperm from wild-type (WT) and the *Ak9* knockout (KO) mice. Scale bar: 10 μm. **(b)** Ultrastructural analysis at the mid-piece of the flagella from the *Ak9* KO mice. Scale bar: 200 μm. **(c)** Ultrastructural analysis at the principal piece of the flagella from the *Ak9* KO mice. Scale bar: 100 μm. **(d)** Percentages of motile spermatozoa in the cauda epididymidis from the wild-type and *Ak9* KO mice. **(e)** Changes in the nucleotide metabolites in the spermatozoa from *Ak9* KO mice compared with WT controls. **(f)** Changes in the glycolytic metabolites in the spermatozoa from *Ak9* KO mice compared with WT controls. **(g)** The percentages of β-ATP phosphoryl labelled with ^{18}O in the spermatozoa from the WT and *Ak9* KO mice. **(h)** The percentages of the 2 PN rate (% of 2PN/total) and birth rate (% of live offspring/transferred embryos) of intracytoplasmic sperm injection (ICSI) of the WT and *Ak9* KO mice. (*p < 0.05, **p < 0.01, ***p < 0.001).

phenotypic analysis revealed that men harbouring bi-allelic *AK9* mutations exhibited typical asthenozoospermia phenotypes, including an extremely lower percentage of the total and progressive sperm motility.

In addition to its energetic function, AK plays a distinct signalling role through the generation of AMP and the activation of AMP-dependent processes, including adenosine production.[68,69] We observed a significant reduction in AMP in the spermatozoa of *AK9*-deficient patients, accompanied by a reduction in other nucleotides of different compositions. This may be due to the deficiency of *AK9* affecting the balance of adenosine homeostasis within the spermatozoa, leading to impaired AMP production, which in turn affects the metabolism of other adenosines in the spermatozoa.

In addition to precise energy metabolism, the impeccable structure of the flagella is essential for sperm motility. Sperm morphological defects are a factor in asthenozoospermia, the most severe of which is MMAF, which attains accessory fibre of the flagellum (69, 70) (68, 69); however, asthenozoospermia can also be caused by genetic mutations that affect the structure or function of the axoneme, with or without concomitant

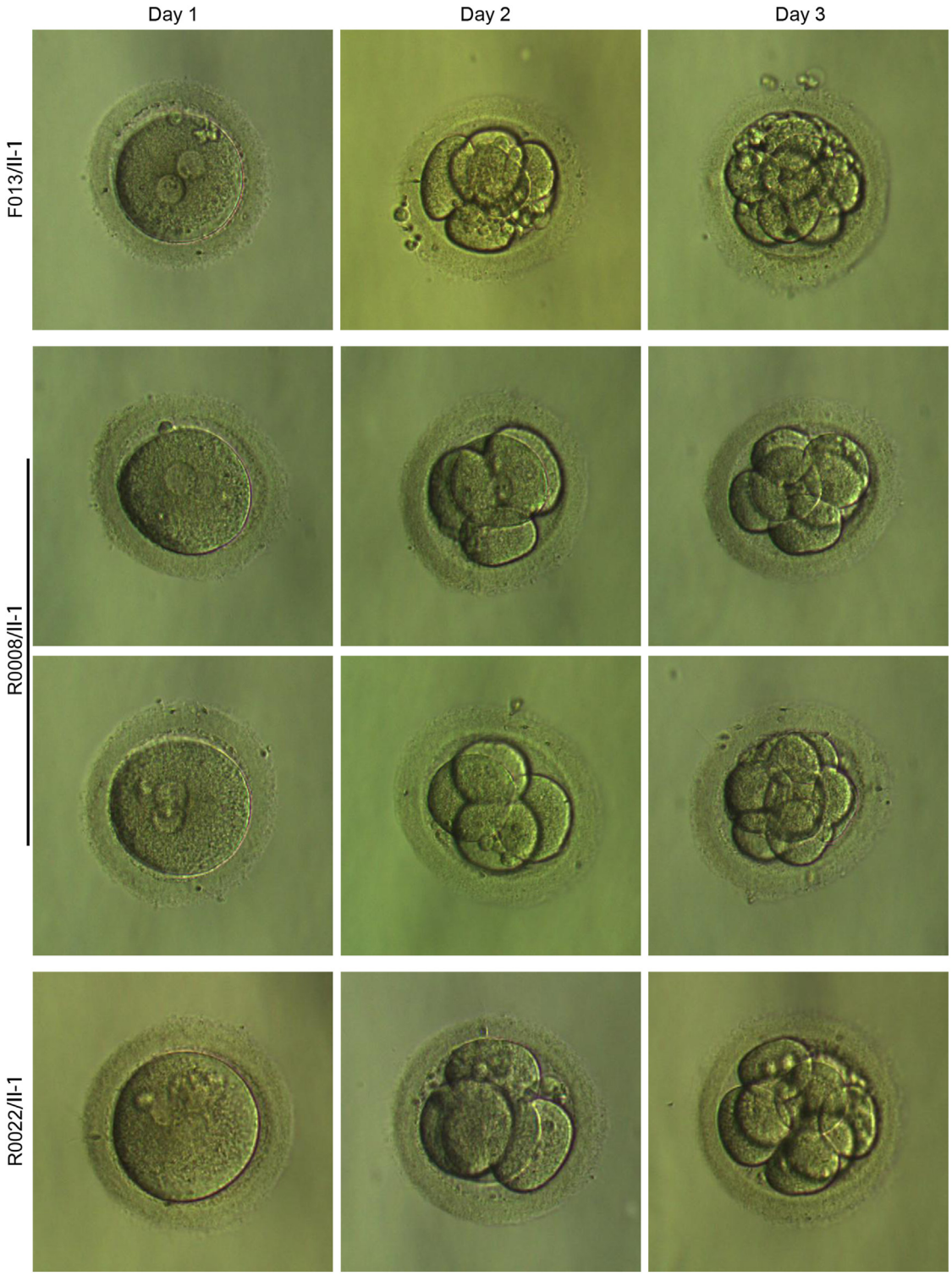

Fig. 6: Morphology of embryogenesis for the implanted embryos. The embryogenesis of the *AK9* mutated patients on day 1, day 2, and day 3.

respiratory cilia impairment.[70,71] In MMAF cases, mutations in genes that are involved in the structure of the flagella, such as *DNAH1*,[72] *AKAP4*,[73] and *SPEF2*,[37] lead to asthenozoospermia. Previous research has indicated that mutations in *AK1* or *AK2* cause chronic haemolytic anaemia and reticular dysgenesis in humans, respectively, and mutations in *AK7* cause primary ciliary dyskinesia or MMAF.[31,74–77] Notably, the results of Papanicolaou staining, SEM, and TEM analysis of sperm indicated that sperm morphology and the architecture of the axoneme running through the flagella did not show a significant difference in men harbouring bi-allelic *AK9* mutations and *Ak9*-null mice. In addition, clinical examinations demonstrated that none of the patients displayed PCD-related symptoms. These clinical symptoms may be because *AK9* is primarily expressed in the testes. Therefore, asthenozoospermia caused by bi-allelic *AK9* mutations may not be caused by abnormalities in the structure of the flagella, but instead by abnormal energy metabolism.

AKs are one of the most fascinating enzymes and are enriched in tissues with a high energy demand,[78] and are responsible for approximately 31% of the non-mitochondrial ATP regeneration in sea urchin spermatozoa flagella and nearly 93% of non-mitochondrial ATP regeneration in the embryonic cilia of sea urchins.[79] Previous studies reported AKs, as the unique hub within the cellular homeostatic network, are involved in multiple energetic and metabolic signalling networks by regulating the homeostasis of nucleotides to convey the energy state.[23] Moreover, it has been demonstrated that AKs can interact with glycolysis enzymes, such as phosphofructokinase, aldolase, phosphoglycerate kinase, and glyceraldehyde phosphate dehydrogenase, in rabbits.[80,81] AK-catalysed reactions have been identified as a promoter of glycolysis by decomposing ATP to alleviate inhibition of glycolysis and providing substrates for glycolysis simultaneously in intact rat muscle.[82] In this study, we identified that bi-allelic *AK9* mutations perturbed the adenosine metabolism, and decreased the ATP, AMP, and ADP concentration. In addition, mutations in *AK9* significantly reduced glycolysis, accompanied by a reduction in lactic acid, but a constant MMP when compared with control subjects, suggesting *AK9* deficiency affected ATP generation via the glycolysis pathway, which led to *AK9*-associated asthenozoospermia.

Consistent with our findings, the dysfunction of glycolysis in sperm is closely related to male infertility caused by asthenozoospermia. Deprivation of genes related to glycolysis, such as *GAPDS*, *PGK2*, and *LDHC*, effectively inhibited mouse sperm motility and led to asthenozoospermia.[83,84] Owing to their unique role in phosphotransfer, AKs can double the energetic potential of ATP. Studies indicated that a deficiency of Ak1 in the muscle and heart of mice inhibited the rate of β-ATP production, decreasing the energy economy.[63,64,85] In this study, we observed a decrease in β-ATP compared with

Patients	F013/II-1	R0008/II-1	R0022/II-1
Male age (years)	31	40	28
Female age (years)	27	31	28
Cycles (n)	1	1	1
Embryo transfer cycles (n)	1	1	1
Oocytes collected (n)	17	11	13
Metaphase II oocytes (n)	12	7	10
Maturation oocyte rate (%)	70.59	63.64	76.92
2 PN (n)	10	6	7
Fertilization rate (%)	83.33	85.71	70
Embryos cleaved at Day 2 (n)	9	5	7
Embryo cleavage rate (%)	90	83.33	100
Day 3 embryos (n)	9	5	7
Day 3 grade A/B embryos (n)	7	4	6
Num. of transferred embryos (n)	1	2	1
Biochemical pregnancy (n)	1	1	1
Clinical pregnancy (n)	1	1	1
Implantation rate (%)	100	50	100
Ectopic pregnancy (n)	0	0	0
Abortion (n)	0	0	0
Delivery (n)	1	1	1
Singletons/Twins	Singletons	Singletons	Singletons
Boy/Girl	Boy	Girl	Girl
Weight (g, range: 2500–4000)	3500	3000	3500

Table 3: **Outcomes of ICSI treatment in the patients with bi-allelic *AK9* mutations.**

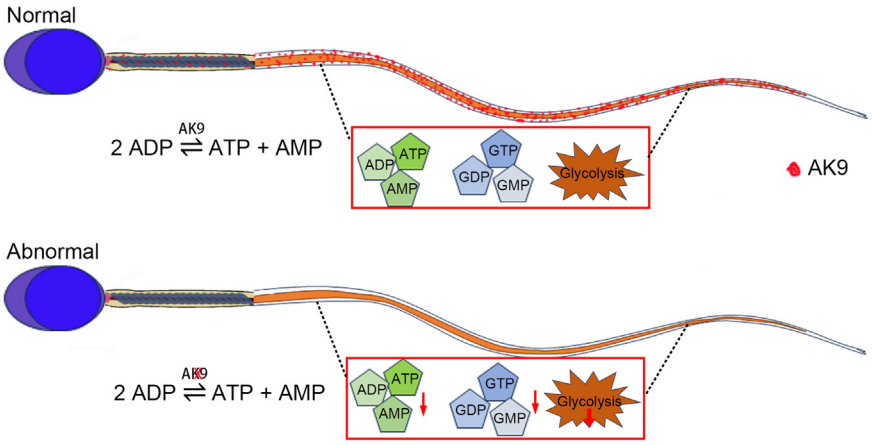

Fig. 7: Schematic model of asthenozoospermia caused by AK9 deficiency.

control individuals, suggesting that AK-catalysed ATP turnover and energy supply play an important role in sperm motility.

Ak9-null male mice display phenotypes similar to those of asthenozoospermia, characterised by markedly decreased sperm motility. *Ak9*-null male mice exhibited regular spermatogenesis in the testes, normal sperm counts, and natural sperm architecture. Consistently, sperm with the *Ak9* deletion were quite sluggish and there was a decreased percentage of progressive sperm. These observations indicated that *Ak9* plays an indispensable role in sperm motility and male fertility.

The proteins AK1 and AK2 are accessory structures in the mouse sperm flagellum.[19] AK1 is expressed in post-meiotic round and elongated spermatids in the mouse testis and mature sperm in the epididymis. *AK1* deletion does not induce reproductive defects under physiological conditions, but can affect sperm motility under energy stress in mice.[28] The AK4 protein participates in the proliferation and apoptosis of human spermatogonial stem cells, which is regulated by SPOCD1.[30] Interestingly, mice with *Ak7* deletion exhibited an MMAF-similar phenotype, which may be due to *Ak7* deficiency damaging the expression of A-kinase anchoring proteins, which is an important component of the axoneme.[31] *AK7* defects causing MMAF may be associated with defects in sperm axoneme formation. In this study, we demonstrated that *Ak9* KO does not affect the ultrastructure of the axoneme, suggesting that asthenozoospermia induced by *Ak9* deletion may not be associated with sperm structural defects and that this phenotype is consistent with humans with bi-allelic *AK9* mutations.

With the advent of ICSI, men with asthenozoospermia can be treated, favourable fertilisation and clinical pregnancy rates can be achieved, including in patients with *DNAH1* (with MMAF), *DNAH2* (with MMAF), and *DNAH7* (with asthenozoospermia) mutations.[34,86,87] On the contrary, mitochondrial genetic mutations, such as nicotinamide adenine dinucleotide hydrogen (NADH) dehydrogenase 1 (*ND1*), NADH dehydrogenase 2 (*ND2*), or NADH dehydrogenase 5 (*ND5*), causing asthenozoospermia, negatively affected ICSI outcomes in humans.[88] In this study, ICSI was performed on the patients F013/II-1, R0008/II-1, and R0022/II-1, and all fulfilled a positive pregnancy outcome and fathered a healthy child. Therefore, our findings prove that ICSI should be the prioritized recommendation for patients with *AK9*-associated asthenozoospermia. However, the limitations of our study must be recognized. We have investigated only part of the patients including ICSI treatment. Moreover, the accuracy role of *AK9* needs to be further validated in a cohort that involving larger and more diverse populations.

In conclusion, we identified *AK9* as a gene responsible for asthenozoospermia in humans and mice. The observed effects of the AK9 protein on nucleotide homeostasis and the energy metabolic network suggest that AK9 is an indispensable component of sperm motility (Fig. 7). Furthermore, we demonstrated that ICSI is an effective method to rescue *AK9*-associated male infertility. Therefore, our findings not only extend the spectrum of aetiological genes involved in asthenozoospermia, but also provides a worthy treatment option for *AK9*-associated male infertility.

Contributors

L.L., H.Z., and W.Q. initiated and supervised the project. Y.S. and W.L. performed the experiments, collected the data, and prepared the original draft manuscript. L.O. and Y.C. contributed to data analysis. S. L., H. N., S. G., and L. X. performed the experiments and acquired the data. L. L., H. Z., and W. Q. edited and finalised the manuscript. Y.S. and L.L. have accessed and verified the underlying data. All authors read and approved the final version of the manuscript for submission.

Data sharing statement

All the data appeared in this manuscript is available to others, including Supplementary Files. The data that support the findings of this study

have been deposited in the CNGB Sequence Archive (CNSA) of the China National GeneBank DataBase (CNGBdb) with accession number CNP0004478. The proteomics data have been deposited to the ProteomeXchange Consortium via the iProX partner repository with identifier PXD043689.

Declaration of interests

The authors declare no conflict of interest.

Acknowledgements

This work was supported by the National Natural Science Foundation of China (82071697), Medical Innovation Project of Fujian Province (2020-CXB-051), open project of the NHC Key Laboratory of Male Reproduction and Genetics in Guangzhou (KF202004), Medical Research Foundation of Guangdong Province (A2021269), Guangdong Provincial Reproductive Science Institute Innovation Team grants (C-03), and Outstanding Young Talents Program of Capital Medical University (B2205).

Appendix A. Supplementary data

Supplementary data related to this article can be found at https://doi.org/10.1016/j.ebiom.2023.104798.

References

1 Vander Borght M, Wyns C. Fertility and infertility: definition and epidemiology. *Clin Biochem*. 2018;62:2–10.
2 Dohle GR, Colpi GM, Hargreave TB, et al. EAU guidelines on male infertility. *Eur Urol*. 2005;48(5):703–711.
3 Jiao SY, Yang YH, Chen SR. Molecular genetics of infertility: loss-of-function mutations in humans and corresponding knockout/mutated mice. *Hum Reprod Update*. 2021;27(1):154–189.
4 Chemes HE. Phenotypes of sperm pathology: genetic and acquired forms in infertile men. *J Androl*. 2000;21(6):799–808.
5 Curi SM, Ariagno JI, Chenlo PH, et al. Asthenozoospermia: analysis of a large population. *Arch Androl*. 2003;49(5):343–349.
6 Tu C, Wang W, Hu T, Lu G, Lin G, Tan YQ. Genetic underpinnings of asthenozoospermia. *Best Pract Res Clin Endocrinol Metabol*. 2020;34(6):101472.
7 Pereira R, Sa R, Barros A, Sousa M. Major regulatory mechanisms involved in sperm motility. *Asian J Androl*. 2017;19(1):5–14.
8 Ferramosca A, Zara V. Bioenergetics of mammalian sperm capacitation. *Biomed Res Int*. 2014;2014:902953.
9 Tourmente M, Varea-Sanchez M, Roldan ERS. Faster and more efficient swimming: energy consumption of murine spermatozoa under sperm competitiondagger. *Biol Reprod*. 2019;100(2):420–428.
10 du Plessis SS, Agarwal A, Mohanty G, van der Linde M. Oxidative phosphorylation versus glycolysis: what fuel do spermatozoa use? *Asian J Androl*. 2015;17(2):230–235.
11 Miki K, Qu W, Goulding EH, et al. Glyceraldehyde 3-phosphate dehydrogenase-S, a sperm-specific glycolytic enzyme, is required for sperm motility and male fertility. *Proc Natl Acad Sci U S A*. 2004;101(47):16501–16506.
12 Odet F, Duan C, Willis WD, et al. Expression of the gene for mouse lactate dehydrogenase C (Ldhc) is required for male fertility. *Biol Reprod*. 2008;79(1):26–34.
13 Kuang W, Zhang J, Lan Z, et al. SLC22A14 is a mitochondrial riboflavin transporter required for sperm oxidative phosphorylation and male fertility. *Cell Rep*. 2021;35(3):109025.
14 Narisawa S, Hecht NB, Goldberg E, Boatright KM, Reed JC, Millan JL. Testis-specific cytochrome c-null mice produce functional sperm but undergo early testicular atrophy. *Mol Cell Biol*. 2002;22(15):5554–5562.
15 Jones AR. The antifertility actions of alpha-chlorohydrin in the male. *Life Sci*. 1978;23(16):1625–1645.
16 Jones AR. Antifertility actions of alpha-chlorohydrin in the male. *Aust J Biol Sci*. 1983;36(4):333–350.
17 Williams AC, Ford WC. The role of glucose in supporting motility and capacitation in human spermatozoa. *J Androl*. 2001;22(4):680–695.
18 Ford WC. Glycolysis and sperm motility: does a spoonful of sugar help the flagellum go round? *Hum Reprod Update*. 2006;12(3):269–274.
19 Cao W, Haig-Ladewig L, Gerton GL, Moss SB. Adenylate kinases 1 and 2 are part of the accessory structures in the mouse sperm flagellum. *Biol Reprod*. 2006;75(4):492–500.
20 Ma J, Rahlfs S, Jortzik E, Schirmer RH, Przyborski JM, Becker K. Subcellular localization of adenylate kinases in Plasmodium falciparum. *FEBS Lett*. 2012;586(19):3037–3043.
21 Dzeja PP, Vitkevicius KT, Redfield MM, Burnett JC, Terzic A. Adenylate kinase-catalyzed phosphotransfer in the myocardium : increased contribution in heart failure. *Circ Res*. 1999;84(10):1137–1143.
22 Dzeja PP, Zeleznikar RJ, Goldberg ND. Adenylate kinase: kinetic behavior in intact cells indicates it is integral to multiple cellular processes. *Mol Cell Biochem*. 1998;184(1–2):169–182.
23 Dzeja P, Terzic A. Adenylate kinase and AMP signaling networks: metabolic monitoring, signal communication and body energy sensing. *Int J Mol Sci*. 2009;10(4):1729–1772.
24 Kinukawa M, Nomura M, Vacquier VD. A sea urchin sperm flagellar adenylate kinase with triplicated catalytic domains. *J Biol Chem*. 2007;282(5):2947–2955.
25 Vadnais ML, Cao W, Aghajanian HK, et al. Adenine nucleotide metabolism and a role for AMP in modulating flagellar waveforms in mouse sperm. *Biol Reprod*. 2014;90(6):128.
26 Dougherty GW, Mizuno K, Nothe-Menchen T, et al. CFAP45 deficiency causes situs abnormalities and asthenospermia by disrupting an axonemal adenine nucleotide homeostasis module. *Nat Commun*. 2020;11(1):5520.
27 Panayiotou C, Solaroli N, Karlsson A. The many isoforms of human adenylate kinases. *Int J Biochem Cell Biol*. 2014;49:75–83.
28 Xie M, Zhang G, Zhang H, et al. Adenylate kinase 1 deficiency disrupts mouse sperm motility under conditions of energy stress-dagger. *Biol Reprod*. 2020;103(5):1121–1131.
29 Ito C, Makino T, Mutoh T, Kikkawa M, Toshimori K. The association of ODF4 with AK1 and AK2 in mice is essential for fertility through its contribution to flagellar shape. *Sci Rep*. 2023;13(1):2969.
30 Zhou D, Zhu F, Huang ZH, Zhang H, Fan LQ, Fan JY. SPOC domain-containing protein 1 regulates the proliferation and apoptosis of human spermatogonial stem cells through adenylate kinase 4. *World J Stem Cells*. 2022;14(12):822–838.
31 Lores P, Coutton C, El Khouri E, et al. Homozygous missense mutation L673P in adenylate kinase 7 (AK7) leads to primary male infertility and multiple morphological anomalies of the flagella but not to primary ciliary dyskinesia. *Hum Mol Genet*. 2018;27(7):1196–1211.
32 Xiang M, Wang Y, Xu W, et al. A novel homozygous missense mutation in AK7 causes multiple morphological anomalies of the flagella and oligoasthenoteratozoospermia. *J Assist Reprod Genet*. 2022;39(1):261–266.
33 Amiri M, Conserva F, Panayiotou C, Karlsson A, Solaroli N. The human adenylate kinase 9 is a nucleoside mono- and diphosphate kinase. *Int J Biochem Cell Biol*. 2013;45(5):925–931.
34 Wei X, Sha Y, Wei Z, et al. Bi-allelic mutations in DNAH7 cause asthenozoospermia by impairing the integrality of axoneme structure. *Acta Biochim Biophys Sin (Shanghai)*. 2021;53(10):1300–1309.
35 Goncalves C, Cunha M, Rocha E, et al. Y-chromosome microdeletions in nonobstructive azoospermia and severe oligozoospermia. *Asian J Androl*. 2017;19(3):338–345.
36 Li Y, Sha Y, Wei Z, et al. A familial analysis of two brothers with azoospermia caused by maternal 46,Y, t(X; 1) (q28; q21) chromosomal abnormality. *Andrologia*. 2021;53(1):e13867.
37 Liu W, Sha Y, Li Y, et al. Loss-of-function mutations in SPEF2 cause multiple morphological abnormalities of the sperm flagella (MMAF). *J Med Genet*. 2019;56(10):678–684.
38 Liu W, Wei X, Liu X, et al. Biallelic mutations in ARMC12 cause asthenozoospermia and multiple midpiece defects in humans and mice, 2022 *J Med Genet*. 2023;60(2):154–162.
39 WHO. *WHO laboratory Manual for the examination and processing of human semen*. 5th ed. Cambridge, UK: University Press; 2010:272.
40 WHO. *WHO laboratory Manual for the examination and processing of human semen*. 5th ed. Cambridge, UK: University Press; 2010:292.
41 Amann RP, Waberski D. Computer-assisted sperm analysis (CASA): capabilities and potential developments. *Theriogenology*. 2014;81(1):5–17.e1-3.
42 Okumuş F, Kocamaz F, Özgür ME. Using polynomial modeling for calculation of sperm quality parameters in CASA. *Comput Sci*. 2021;6(3):152–165.
43 Wei X, Liu W, Zhu X, et al. Biallelic mutations in KATNAL2 cause male infertility due to oligo-astheno-teratozoospermia. *Clin Genet*. 2021;100(4):376–385.
44 Sha Y, Liu W, Tang S, et al. TENT5D disruption causes oligoasthenoteratozoospermia and male infertility. *Andrology*. 2023;11(6):1121–1131.

45 Evenson DP. Sperm chromatin structure assay (SCSA(R)) for fertility assessment. *Curr Protoc*. 2022;2(8):e508.
46 Sha YW, Wang X, Xu X, et al. Biallelic mutations in PMFBP1 cause acephalic spermatozoa. *Clin Genet*. 2019;95(2):277–286.
47 Sha YW, Sha YK, Ding L, et al. A successful pregnancy by intracytoplasmic sperm injection using ejaculate sperm from an infertile man with 46, XX/46, XY true hermaphrodite. *Asian J Androl*. 2017;19(6):721–722.
48 Sha Y, Chen Y, Wang X, et al. Biallelic mutations in IQCN, encoding a novel acroplaxome protein, lead to fertilization failure and male infertility with defects in the acrosome and shaping of the spermatid head in humans and mice. *Life Med*. 2023;2(2):lnac050.
49 Depalo R, Jayakrishan K, Garruti G, et al. GnRH agonist versus GnRH antagonist in in vitro fertilization and embryo transfer (IVF/ET). *Reprod Biol Endocrinol*. 2012;10:26.
50 Pinto F, Oliveira C, Cardoso MF, et al. Impact of GnRH ovarian stimulation protocols on intracytoplasmic sperm injection outcomes. *Reprod Biol Endocrinol*. 2009;7:5.
51 Palermo G, Joris H, Devroey P, Van Steirteghem AC. Pregnancies after intracytoplasmic injection of single spermatozoon into an oocyte. *Lancet*. 1992;340(8810):17–18.
52 Van Steirteghem AC, Liu J, Joris H, et al. Higher success rate by intracytoplasmic sperm injection than by subzonal insemination. Report of a second series of 300 consecutive treatment cycles. *Hum Reprod*. 1993;8(7):1055–1060.
53 Van Steirteghem AC, Nagy Z, Joris H, et al. High fertilization and implantation rates after intracytoplasmic sperm injection. *Hum Reprod*. 1993;8(7):1061–1066.
54 Cooper TG, Noonan E, von Eckardstein S, et al. World Health Organization reference values for human semen characteristics. *Hum Reprod Update*. 2010;16(3):231–245.
55 Auger J, Jouannet P, Eustache F. Another look at human sperm morphology. *Hum Reprod*. 2016;31(1):10–23.
56 Almeida S, Rato L, Sousa M, Alves MG, Oliveira PF. Fertility and sperm quality in the aging male. *Curr Pharm Des*. 2017;23(30):4429–4437.
57 Freitas MJ, Vijayaraghavan S, Fardilha M. Signaling mechanisms in mammalian sperm motility. *Biol Reprod*. 2017;96(1):2–12.
58 Galantino-Homer HL, Florman HM, Storey BT, Dobrinski I, Kopf GS. Bovine sperm capacitation: assessment of phosphodiesterase activity and intracellular alkalinization on capacitation-associated protein tyrosine phosphorylation. *Mol Reprod Dev*. 2004;67(4):487–500.
59 Kishi F, Tanizawa Y, Nakazawa A. Isolation and characterization of two types of cDNA for mitochondrial adenylate kinase and their expression in Escherichia coli. *J Biol Chem*. 1987;262(24):11785–11789.
60 Nakazawa A, Yamada M, Tanaka H, Shahjahan M, Tanabe T. Gene structures of three vertebrate adenylate kinase isozymes. *Prog Clin Biol Res*. 1990;344:495–514.
61 Lee Y, Kim JW, Lee SM, et al. Cloning and expression of human adenylate kinase 2 isozymes: differential expression of adenylate kinase 1 and 2 in human muscle tissues. *J Biochem*. 1998;123(1):47–54.
62 Villa H, Perez-Pertejo Y, Garcia-Estrada C, et al. Molecular and functional characterization of adenylate kinase 2 gene from Leishmania donovani. *Eur J Biochem*. 2003;270(21):4339–4347.
63 Janssen E, Dzeja PP, Oerlemans F, et al. Adenylate kinase 1 gene deletion disrupts muscle energetic economy despite metabolic rearrangement. *EMBO J*. 2000;19(23):6371–6381.
64 Pucar D, Bast P, Gumina RJ, et al. Adenylate kinase AK1 knockout heart: energetics and functional performance under ischemia-reperfusion. *Am J Physiol Heart Circ Physiol*. 2002;283(2):H776–H782.
65 Schoff PK, Cheetham J, Lardy HA. Adenylate kinase activity in ejaculated bovine sperm flagella. *J Biol Chem*. 1989;264(11):6086–6091.
66 Kinukawa M, Vacquier VD. Recombinant sea urchin flagellar adenylate kinase. *J Biochem*. 2007;142(4):501–506.
67 Guo Y, Jiang W, Yu W, et al. Proteomics analysis of asthenozoospermia and identification of glucose-6-phosphate isomerase as an important enzyme for sperm motility. *J Proteomics*. 2019;208:103478.
68 Kroll K, Decking UK, Dreikorn K, Schrader J. Rapid turnover of the AMP-adenosine metabolic cycle in the Guinea pig heart. *Circ Res*. 1993;73(5):846–856.
69 Dzeja PP, Terzic A. Phosphotransfer reactions in the regulation of ATP-sensitive K+ channels. *FASEB J*. 1998;12(7):523–529.
70 Pereira R, Oliveira J, Ferraz L, Barros A, Santos R, Sousa M. Mutation analysis in patients with total sperm immotility. *J Assist Reprod Genet*. 2015;32(6):893–902.
71 Pereira R, Sousa M. Morphological and molecular bases of male infertility: a closer look at sperm flagellum. *Genes (Basel)*. 2023;14(2):383.
72 Sha Y, Yang X, Mei L, et al. DNAH1 gene mutations and their potential association with dysplasia of the sperm fibrous sheath and infertility in the Han Chinese population. *Fertil Steril*. 2017;107(6):1312–1318.e2.
73 Miki K, Willis WD, Brown PR, Goulding EH, Fulcher KD, Eddy EM. Targeted disruption of the Akap4 gene causes defects in sperm flagellum and motility. *Dev Biol*. 2002;248(2):331–342.
74 Lagresle-Peyrou C, Six EM, Picard C, et al. Human adenylate kinase 2 deficiency causes a profound hematopoietic defect associated with sensorineural deafness. *Nat Genet*. 2009;41(1):106–111.
75 Pannicke U, Honig M, Hess I, et al. Reticular dysgenesis (aleukocytosis) is caused by mutations in the gene encoding mitochondrial adenylate kinase 2. *Nat Genet*. 2009;41(1):101–105.
76 Fernandez-Gonzalez A, Kourembanas S, Wyatt TA, Mitsialis SA. Mutation of murine adenylate kinase 7 underlies a primary ciliary dyskinesia phenotype. *Am J Respir Cell Mol Biol*. 2009;40(3):305–313.
77 Matsuura S, Igarashi M, Tanizawa Y, et al. Human adenylate kinase deficiency associated with hemolytic anemia. A single base substitution affecting solubility and catalytic activity of the cytosolic adenylate kinase. *J Biol Chem*. 1989;264(17):10148–10155.
78 Alhusani A, Obaid A, Blom HJ, Wedell A, Alfadhel M. Adenosine kinase deficiency: report and review. *Neuropediatrics*. 2019;50(1):46–50.
79 Kinukawa M, Vacquier VD. Adenylate kinase in sea urchin embryonic cilia. *Cell Motil Cytoskeleton*. 2007;64(4):310–319.
80 Ovadi J, Keleti T. Kinetic evidence for interaction between aldolase and D-glyceraldehyde-3-phosphate dehydrogenase. *Eur J Biochem*. 1978;85(1):157–161.
81 Oguchi M, Meriwether BP, Park JH. Interaction between adenosine triphosphate and glyceraldehyde 3-phosphate dehydrogenase. 3. Mechanism of action and metabolic control of the enzyme under simulated in vivo conditions. *J Biol Chem*. 1973;248(16):5562–5570.
82 Zeleznikar RJ, Dzeja PP, Goldberg ND. Adenylate kinase-catalyzed phosphoryl transfer couples ATP utilization with its generation by glycolysis in intact muscle. *J Biol Chem*. 1995;270(13):7311–7319.
83 Odet F, Gabel S, London RE, Goldberg E, Eddy EM. Glycolysis and mitochondrial respiration in mouse LDHC-null sperm. *Biol Reprod*. 2013;88(4):95.
84 Danshina PV, Geyer CB, Dai Q, et al. Phosphoglycerate kinase 2 (PGK2) is essential for sperm function and male fertility in mice. *Biol Reprod*. 2010;82(1):136–145.
85 Pucar D, Janssen E, Dzeja PP, et al. Compromised energetics in the adenylate kinase AK1 gene knockout heart under metabolic stress. *J Biol Chem*. 2000;275(52):41424–41429.
86 Li Y, Sha Y, Wang X, et al. DNAH2 is a novel candidate gene associated with multiple morphological abnormalities of the sperm flagella. *Clin Genet*. 2019;95(5):590–600.
87 Wambergue C, Zouari R, Fourati Ben Mustapha S, et al. Patients with multiple morphological abnormalities of the sperm flagella due to DNAH1 mutations have a good prognosis following intracytoplasmic sperm injection. *Hum Reprod*. 2016;31(6):1164–1172.
88 Al Smadi MA, Hammadeh ME, Solomayer E, et al. Impact of mitochondrial genetic variants in ND1, ND2, ND5, and ND6 genes on sperm motility and intracytoplasmic sperm injection (ICSI) outcomes. *Reprod Sci*. 2021;28(5):1540–1555.